

Uncovering Nonconventional and Conventional Hydrogen Bonds in Oligosaccharides through NMR Experiments and Molecular Modeling: Application to Sialyl Lewis-X

Marcos D. Battistel,[†] Hugo F. Azurmendi,[†] Martin Frank,[‡] and Darón I. Freedberg^{*,†}

[†]Laboratory of Bacterial Polysaccharides, Food and Drug Administration, 10903 New Hampshire Avenue, Silver Spring, Maryland 20903, United States

[‡]Biognos AB, Generatorsgatan 1, 41705 Gothenburg, Sweden

S Supporting Information

ABSTRACT: We describe the direct NMR detection of a C–H...O nonconventional hydrogen bond (Hbond) and provide experimental and theoretical evidence for conventional Hbonds in the pentasaccharide sialyl Lewis-X (sLe^X-5) between 5 and 37 °C in water. Extensive NMR structural studies together with molecular dynamics simulations offer strong evidence for significant local dynamics in the Le^X core and for previously undetected conventional Hbonds in rapid equilibrium that modulate structure. These NMR studies also showed temperature-dependent ¹H and ¹³C line broadening. The resulting model emerging from this study is more complex than a simple rigid core description of Le^X-like molecules and improves our understanding of stabilizing interactions in glycans.

Hydrogen bonds (Hbonds) are central interactions in biomolecules, stabilizing protein and nucleic acid folds and tertiary structure. Hbonding in glycans has been hypothesized, but is difficult to detect in H₂O. Nonetheless, methods exist to detect Hbonds in H₂O.^{1,2} Recently, a nonconventional Hbond, where an aliphatic H is the Hbond donor, was proposed to exist in Lewis-X (Le^X) from NMR chemical shifts and DFT calculations.³ Yet, experimental evidence for this Hbond is lacking. Nonconventional Hbonds in glycans have been observed in DMSO.⁴ In this report, we provide direct NMR evidence for this Hbond in the sialyl Lewis-X pentasaccharide (sLe^X-5) in H₂O (Figure 1A). Moreover, we performed an extensive temperature-dependent NMR structural study in conjunction with molecular dynamics (MD) simulations to provide novel evidence for two conventional Hbonds in rapid equilibrium. The results improve our understanding of stabilizing interactions in glycans in aqueous solution.

We detected a nonconventional C–H...O Hbond in sLe^X-5 using long-range HSQC (lr-HSQC) experiments, which allow efficient ¹H, ¹³C coherence transfer (SI), like those expected for Hbonds. As Hbond signals are sensitive to temperature,⁶ we performed experiments at various temperatures to find the best condition for detection. Figure 1B–D show the lr-HSQC correlation signal observed for (Gal{IV}H1, Fuc{III}C5) at three different conditions. Figure 1B shows detection with a standard probe at 700 MHz. The signal-to-noise ratio (SNR) is

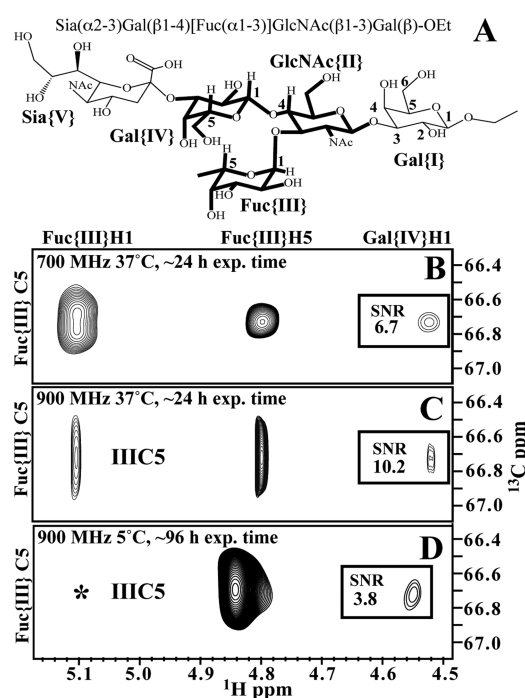


Figure 1. sLe^X-5 chemical structure (A) and ¹H,¹³C lr-HSQC strips showing the Gal{IV}H1-Fuc{III}C5 correlation (B–D), with its corresponding SNR. Experimental conditions are indicated in each panel. In (D) the missing Fuc{III}H1–C5 correlation (*) and the residual HOD signal overlap, and both are filtered during processing.

low and at 5 °C the peak was not visible with this instrument (data not shown). We verified the correlation under similar conditions in a 900 MHz spectrometer with cryoprobe, where the SNR improved by ~50% at 37 °C (Figure 1C), partly due to a smaller exchange contribution to T₂. At 5 °C (Figure 1D) the chemical shift of Fuc{III}H5 changes and the ¹H line broadens significantly; even 96 h acquisition resulted in significantly lower SNR than 24 h at 37 °C. Together, the broadening and chemical shift changes are consistent with variable dynamics for the Le^X core.⁷ After 9 days of data collection at 850 MHz (1536 scans per t1 increment) and 37 °C, we observed two additional

Received: April 13, 2015

Published: October 1, 2015

correlations, Fuc{III}H5-Gal{IV}C1 (SNR 11:1) and Fuc{III}-H5-GlcNAc{II}C4 (SNR 13:1) (Figure S3).

The through-bond path for the (Gal{IV}H1, Fuc{III}C5) signal is eight covalent-bonds, far too long to allow for magnetization transfer through J -coupling to occur (SI). Thus, a shorter Hbond-mediated pathway is required. The observed inter-residue cross peaks enable the confident identification of Fuc{III}H5 as the Hbond donor group, as previously predicted.³ However, the Hbond acceptor could not be uniquely identified. Thus, the Hbond pathway must be derived instead from structural models, consistent with experimental observations.

Reported structures of sLe^X tetrasaccharide^{8–11} and Le^X trisaccharide^{10,12–14} are consistent with a relatively rigid Le^X core ($\{II\} \rightarrow [\{III\},\{IV\}]$),^{15–17} and flexible end-groups in the case of sLe^X-5 . Because of the additional galactose residue and the temperature range used for Hbond NMR measurements in this work, we independently characterized the structure of sLe^X-5 (Figure 1A) by both MD and NMR at various temperatures (SI). The energy maps derived from MD¹⁸ (Figure 2) summarize the results at 37 °C using conformer populations for each of the four linkages in sLe^X-5 . The low-energy regions for the Le^X core linkages consist of single minima with limited excursions of (ϕ, ψ) torsions, but allowing for relatively wide variations of ca. $\pm 30^\circ$ away from the minima. All experimental unbound and most protein-bound structures reported for the Le^X core fall within these limits (SI).^{3,7,10,12–14,19} In contrast, linkages for Gal{I} and Sia{V} are more flexible with multiple energy minima (Figure S12). Energy barriers for exchange among conformers range from 1 to 2 kcal/mol and frequent transitions occur (Figure S13).

Parallel to MD, NMR data yielded restraints for simulated annealing calculations resulting in ensembles of 200 structures at each of four different temperatures (Figure S8). The Le^X core in Figure 3A contains the four representative structures for each temperature showing little dispersion. Sia{V} instead is very dispersed; for clarity we only show three of them (gray/magenta/yellow), consistent with both NMR and the energy minima for the $\{V\} \rightarrow \{IV\}$ linkage. Similarly, two (ϕ, ψ) values are required to properly represent Gal{I} (cyan/teal) consistent with the results for the $\{II\} \rightarrow \{I\}$ linkage. Further, NMR data at -10°C provided additional hydroxyl ^1H NOEs that improved

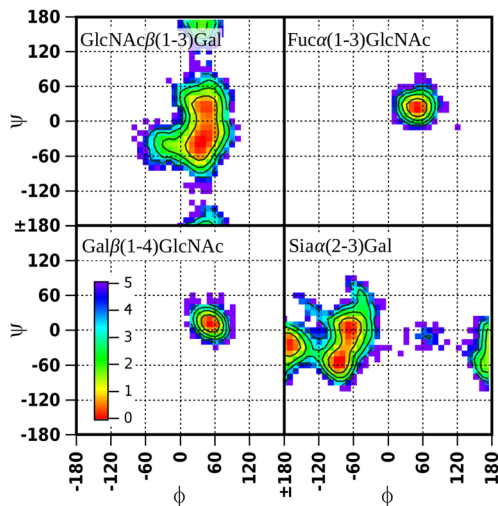


Figure 2. Energy (ϕ, ψ) maps for sLe^X-5 linkages from a 500 ns MD simulation in explicit water at 37 °C. Color scale is in kcal/mol derived from population ratios.¹⁵

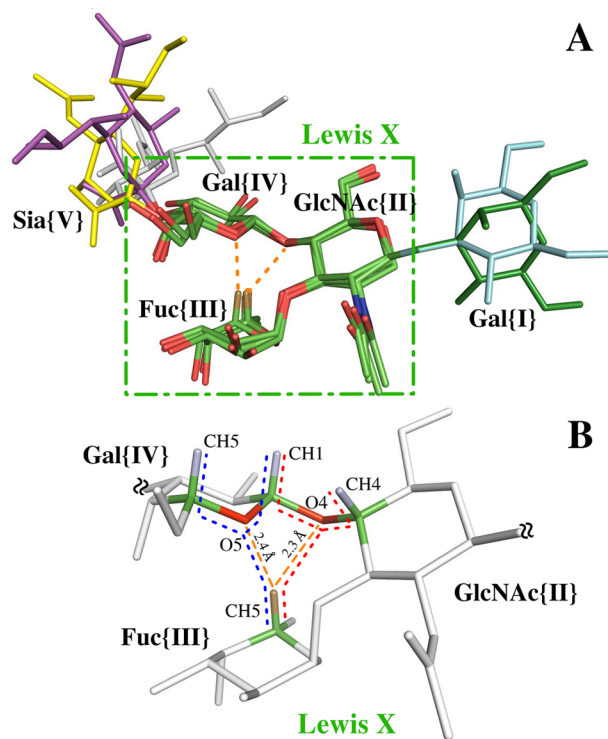


Figure 3. NMR derived structures of sLe^X-5 . (A) Representative NMR structures at $-10, 5, 15,$ and 37°C (see text). (B) Le^X core with Fuc{III}H5 distances to Gal{IV}O5 and GlcNAc{II}O4. Blue and red dashed lines trace possible magnetization transfer pathways.

structure precision. Structures derived with hydroxyl ^1H NOE restraints favored a single conformation for the $\{II\} \rightarrow \{I\}$ linkage with (ϕ, ψ) torsion values $\sim(60^\circ, -30^\circ)$ (Figures S8 and S9).

With the Le^X core structure well described, it is possible to analyze the available pathways for magnetization transfer (Figure 3B, red and blue dots) leading to the observed NMR signals. The three signals observed can be interpreted equally well as resulting from $^4J_{\text{CH}}$ or $^2J_{\text{CH}}$ with either Gal{IV}O5 or GlcNAc{II}O4 as acceptor. The average distances between Fuc{III}H5 and its nearest oxygen neighbors, in the NMR derived structure at 37 °C, are Gal{IV}O5 (2.4 ± 0.2) and GlcNAc{II}O4 (2.3 ± 0.2). The average distance from MD simulations agrees with the former (2.6 ± 0.3 for Fuc{III}H5-Gal{IV}O5), but it is larger for the latter (3.2 ± 0.4 for Fuc{III}H5-GlcNAc{II}O4). The distance and average C–H–O angles ($160 \pm 10^\circ$ for the former vs $134 \pm 10^\circ$ for the latter) clearly favor the blue Hbond pathway over the red. The absence of a correlation from Fuc{III}C/H5 to GlcNAc{II}H/C4 on all but extremely lengthy experiments supports this hypothesis as well. Nevertheless, some Hbond character cannot be totally dismissed for Fuc{III}CH5...GlcNAc{II}O4, as directionality is less determinant in weak Hbonds.²⁰ This would allow for weak magnetization transfer through this pathway to reinforce transfers to/from Gal{IV}C/H1, but not sufficient to produce correlations to GlcNAc{II}C/H4. Notably, MD yields a very stable Le^X core conformation and a C–H...O geometry consistent with an Hbond for Fuc{III}CH5...Gal{IV}O5, despite the force-field defined value of zero partial charge for aliphatic hydrogen atoms (SI). Consequently, the Le^X core may not require the existence of a CH...O in order to maintain its rather rigid global minimum conformation. Yet, our NMR results clearly show that the CH...O bond exists in

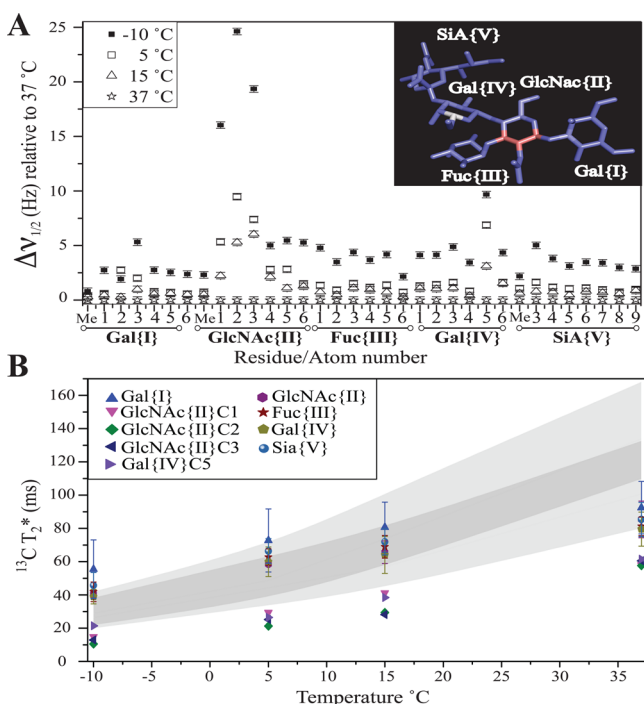


Figure 4. (A) ^{13}C line width changes ($\Delta\nu_{1/2}$) with temperature for sLe^X-5, relative to $\nu_{1/2}$ at 37 °C. Inset: sLe^X-5 structure color coded by $\Delta\nu_{1/2}$ between 37 and -10 °C (low to high as blue–white–red gradient). (B) Estimated T_2^* values derived from $\nu_{1/2}$. The gray shading area indicates expected T_2 values for an anisotropically tumbling sLe^X-5 (SI).

sLe^X-5, which is in general agreement with Zierke et al.³ We also performed QM calculations on model systems and could reproduce the reported energy of -1.7 kcal/mol for the CH...O bond (Figure S16). However, the calculated energy of the CH...O Hbond depends strongly on models and the level of theory used (Figure S17). The presence and magnitude of this Hbond could be gauged by substituting a ^2H for Fuc{III}H5, which should introduce an isotope effect on Fuc{III}C5, Gal{IV}C5, and GlcNAc{II}C4.

Having identified Fuc{III}C/H5...Gal{IV}O5 as the most likely magnetization transfer path in sLe^X-5 in Ir-HSQC experiments, the absence of a Fuc{III}H5 to Gal{IV}C5 correlation also needs to be explained. Small through-Hbond coupling constant together with short ^{13}C T_2^* values are the most plausible explanation for peaks' absence. NMR signals for carbon atoms C1, C2, and C3 in GlcNAc{II}, and C5 in Gal{IV} (Figure 4A) are 2- to 3-fold broader than the expected values at -10 °C (Figure S4B). The expected ^{13}C line width ($\nu_{1/2}$) and T_2 change with temperature for sLe^X-5 was computed based on the experimental sample viscosity at different temperatures and an axially symmetric model for sLe^X-5.²¹ Figure 4B shows T_2^* values derived from $\nu_{1/2}$ and the calculated ^{13}C T_2^* for an anisotropic model of sLe^X-5. The observed temperature dependence of ^{13}C $\nu_{1/2}$ (and T_2^*), for those atoms' signals, clearly indicate conformational motion in the Le^X core. This last observation together with the chemical shift change at 900 MHz at 5 °C suggests that motion decreases the SNR of expected correlations and explains the absence of a Fuc{III}C5/H5 to Gal{IV}H5/C5 correlation at high temperatures. It also explains the absence of any Hbond correlation at 700 MHz below 5 °C.

The remarkable signal broadening in the GlcNAc residue is seen for carbons clustered around the *N*-acetyl group (C1, C2, and C3). No similar effect is observed for carbons of the Sia

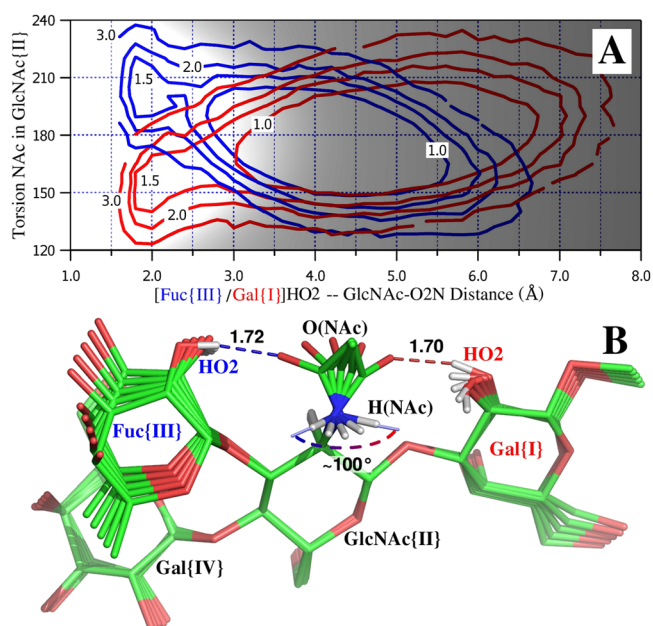


Figure 5. Hbond interactions of NAc group in GlcNAc{II}. (A) Energy map of NAc torsion angle (H2-C2-N2-O2N) correlated with distances to HO2 atoms in Fuc{III} (blue) and Gal{I} (red). The region of Hbond interaction is highlighted. (B) Span of the NAc sweep between conformations with O(NAc) Hbonded to HO2 in Fuc{III} and Gal{I}, respectively.

residue at equivalent locations relative to the NAc group (C4, C5, and C6), indicative of different dynamics for both *N*-acetyl groups. Comparisons of conformational energy maps for linkages like those in Figure 2 with maps from lower temperature MD runs showed only minor differences and could not explain the changes observed in ^{13}C $\nu_{1/2}$ (Figure S12).

From changes in ^{13}C line widths with temperature, motion on the millisecond time scale can be inferred. MD simulations of that duration are currently beyond reach and for high-energy states do not provide accurate exchange rates, but MD can be used to identify interactions leading to the differential dynamics suggested by the ^{13}C $\nu_{1/2}$. An Hbond statistical analysis of MD trajectories was performed, with conventional Hbond donor-acceptor limits for distances and angles of 3.4 Å and 130°, respectively (SI). Sia{V} shows significant inter-residue contacts with Gal{IV} and less frequent contacts with Fuc{III} (Figure S14). While these contacts do not affect the Le^X core structure, they may be important for function. In addition, GlcNAc{II}-O2N is revealed as an acceptor for two donors located at opposite sides of the NAc group: Fuc{III}OH2 and Gal{I}OH2. The impact of these interactions on local dynamics is uncovered when plotting donor hydrogen to acceptor distances vs NAc torsion (Figure 5A), where both Hbond interactions increase the degree of the natural excursion of the NAc torsion angle away from equilibrium by about 20° in each direction. Moreover, the population fraction in the MD trajectory at 37 °C with donor-acceptor distances less than 3.4 Å from O2N to either OH was ~9%. As expected, this fraction decreases with temperature and likely affects the dynamics of the NAc group. Figure 5B illustrates the span of the sweep performed by the NAc group when going from one Hbond to the other. The two extreme structures in Hbond interactions were extracted from the MD trajectory. The intermediate models were obtained following an energy-minimized path compatible with the trajectory, highlighting the

local torsional strain caused in the NAc anchoring ring bonds leading to differential local dynamics. Although the movement is stochastic, the extreme conformations are reached thousands of times during NMR experiments. Experimental support for this motion is found in the increase in GlcNAc{II}HN-HC2's $^3J_{\text{HH}}$ coupling constant, from 9.4 Hz ($-10\text{ }^\circ\text{C}$) to 10.2 Hz ($37\text{ }^\circ\text{C}$). This variation in $^3J_{\text{HH}}$ translates to a GlcNAc{II}HN-HC2 torsion angle difference of ca. $\pm 20^\circ$ (from 158 at $-10\text{ }^\circ\text{C}$ to 180° at $37\text{ }^\circ\text{C}$). No such change in $^3J_{\text{HH}}$ is observed for the Sia NAc group (Table S1). Similar motion of the NAc group in aminosugars was attributed to the NAc group acting as a gatekeeper for transitions in glycosidic torsions.²²

We presented direct NMR evidence for nonconventional and indirect evidence for conventional Hbonds in sLe^X-5 at physiological and lower temperatures. ^{13}C $\nu_{1/2}$ measurements coupled with MD Hbond analysis uncovered details of the Le^X core dynamics, not revealed by analysis of ring linkages. This study opens the door for future detection of Hbonding in glycans and also suggests that higher magnetic fields, together with temperature-dependence studies and accompanied by computational methods, as suggested,²³ will yield new insights into the structure and function of glycans.

■ ASSOCIATED CONTENT

📄 Supporting Information

The Supporting Information is available free of charge on the ACS Publications website at DOI: 10.1021/jacs.5b03824.

Materials and methods, supporting figures, MD simulations, NMR structure calculations, temperature-dependent NMR spectra (PDF)

Observed NOEs and NOEs vs temperature (XLSX)

NMR assignments with long-range correlations (XLSX)

■ AUTHOR INFORMATION

Corresponding Author

*daron.freedberg@fda.hhs.gov

Notes

The authors declare no competing financial interest.

■ ACKNOWLEDGMENTS

We are grateful to Jim Paulson for the sLe^X-5 sample, Nico Tjandra (NIH) for use of the 900 MHz NMR spectrometer, David Keire (CDER) for use of the 850 MHz NMR Spectrometer, Ross Walker (San Diego Supercomputing Center) for helping us set up a GPU for M.D., and Dennis Torchia (NIH) for helpful discussions.

■ REFERENCES

- (1) Battistel, M. D.; Shangold, M.; Trinh, L.; Shiloach, J.; Freedberg, D. *I. J. Am. Chem. Soc.* **2012**, *134*, 10717.
- (2) Battistel, M. D.; Pendrill, R.; Widmalm, G.; Freedberg, D. *I. J. Phys. Chem. B* **2013**, *117*, 4860.
- (3) Zierke, M.; Smiesko, M.; Rabbani, S.; Aeschbacher, T.; Cutting, B.; Allain, F. H. T.; Schubert, M.; Ernst, B. *J. Am. Chem. Soc.* **2013**, *135*, 13464.
- (4) Chen, C. S.; Yu, Y. P.; Lin, B. C.; Gervay-Hague, J.; Fang, J. M.; Hsu, C. P.; Wu, S. H. *Eur. J. Org. Chem.* **2009**, *2009*, 3351.
- (5) Paulson, J. C.; Perez, M. S.; Gaeta, A.; Ratcliffe, R. M. Cytel Corporation. US Patent 5753631, 1998.
- (6) Sinciska, W.; Adams, B.; Lerner, L. *Carbohydr. Res.* **1993**, *242*, 29.
- (7) Pederson, K.; Mitchell, D. A.; Prestegard, J. H. *Biochemistry* **2014**, *53*, 5700.

(8) Lin, Y. C.; Hummel, C. W.; Huang, D. H.; Ichikawa, Y.; Nicolaou, K. C.; Wong, C. H. *J. Am. Chem. Soc.* **1992**, *114*, 5452.

(9) Rutherford, T. J.; Spackman, D. G.; Simpson, P. J.; Homans, S. W. *Glycobiology* **1994**, *4*, 59.

(10) Pérez, S.; Mouhous-Riou, N.; Nifant'ev, N. E.; Tsvetkov, Y. E.; Bachet, B.; Imberty, A. *Glycobiology* **1996**, *6*, 537.

(11) Veluraja, K.; Margulis, C. J. *J. Biomol. Struct. Dyn.* **2005**, *23*, 101.

(12) Wormald, M. R.; Edge, C. J.; Dwek, R. A. *Biochem. Biophys. Res. Commun.* **1991**, *180*, 1214.

(13) Miller, K. E.; Mukhopadhyay, C.; Cagas, P.; Bush, C. A. *Biochemistry* **1992**, *31*, 6703.

(14) Azurmendi, H. F.; Martin-Pastor, M.; Bush, C. A. *Biopolymers* **2002**, *63*, 89.

(15) Guo, Y.; Feinberg, H.; Conroy, E.; Mitchell, D. A.; Alvarez, R.; Blixt, O.; Taylor, M. E.; Weis, W. I.; Drickamer, K. *Nat. Struct. Mol. Biol.* **2004**, *11*, 591.

(16) van Roon, A.-M. M.; Pannu, N. S.; de Vrind, J. P. M.; van der Marel, G. A.; van Boom, J. H.; Hokke, C. H.; Deelder, A. M.; Abrahams, J. P. *Structure* **2004**, *12*, 1227.

(17) Feinberg, H.; Taylor, M. E.; Weis, W. I. *J. Biol. Chem.* **2007**, *282*, 17250.

(18) Frank, M.; Lutteke, T.; von der Lieth, C. W. *Nucleic Acids Res.* **2007**, *35*, 287.

(19) Ishida, T. *J. Phys. Chem. B* **2010**, *114*, 3950.

(20) Steiner, T. *Chem. Commun.* **1997**, 727.

(21) Ortega, A.; Amoros, D.; Garcia de la Torre, J. *Biophys. J.* **2011**, *101*, 892.

(22) Pendrill, R.; Jonsson, H. M.; Widmalm, G. *Pure Appl. Chem.* **2013**, *85*, 1759.

(23) Toukach, F. V.; Ananikov, V. P. *Chem. Soc. Rev.* **2013**, *42*, 8376.